

CityLight: A Universal Model for Coordinated Traffic Signal Control in City-scale Heterogeneous Intersections

Jinwei Zeng, Chao Yu, Xinyi Yang, Wenxuan Ao, Qianye Hao, Jian Yuan, Yong Li, Yu Wang, Huazhong Yang

Department of Electronic Engineering, Tsinghua University

Abstract

The increasingly severe congestion problem in modern cities strengthens the significance of developing city-scale traffic signal control (TSC) methods for traffic efficiency enhancement. While reinforcement learning has been widely explored in TSC, most of them still target small-scale optimization and cannot directly scale to the city level due to unbearable resource demand. Only a few of them manage to tackle city-level optimization, namely a thousand-scale optimization, by incorporating parameter-sharing mechanisms, but hardly have they fully tackled the heterogeneity of intersections and intricate between-intersection interactions inherent in real-world city road networks. Moreover, their evaluations were limited to regular and structured road networks, possibly obscuring their shortcomings in dealing with complex road networks. To fill in the gap, we follow the parameter-sharing paradigm and target city-level coordinated traffic signal control accounting for the intricacy of real-world road networks, aiming to solve the two important challenges: inconsistency of inner state representations for intersections heterogeneous in configuration, scale, and orders of available traffic phases; intricacy of impacts from neighborhood intersections that have various relative traffic relationships due to inconsistent phase orders and diverse relative positioning. Our method, CityLight, thereby features a universal representation module that not only aligns the state representations of intersections by reindexing their phases based on their semantics and designing heterogeneity-preserving observations, but also encodes the narrowed relative traffic relation types to project the neighborhood intersections onto a uniform relative traffic impact space. We further attentively fuse neighborhood representations based on their competing relations and incorporate neighborhood-integrated rewards to boost coordination. Extensive experiments on five datasets with hundreds to tens of thousands of intersections collected from the real world validate the surprising effectiveness and generalizability of CityLight, with an overall performance gain of 11.68% and a 22.59% improvement in transfer scenarios in terms of throughput. Our codes and datasets are released: <https://anonymous.4open.science/r/CityLight-CB80>.

Introduction

Traffic signal control (TSC) has been recognized as an effective measure for improving traffic efficiency (Chien, Kim,

and Daniel 2006). Given the continuously severing traffic congestion in modern cities (Afrin and Yodo 2020), it is crucial to develop traffic signal control methods that comprehensively optimize signals at the city scale to approach optimal city-wide control. However, as the real-world road network exhibits significant variability across the city, particularly in terms of structure and density, real-life intersections are unevenly distributed with varying configurations (Fig 1(b)) instead of being ideally gridded distributed (Fig 1(a)). Therefore, the city-level traffic signal control problem encompasses the inherent need to tackle heterogeneous intersections and achieve coordination among intricate interconnections.

With the capacity to learn from environmental feedback and adaptively improve decision-making policies, reinforcement learning has been widely explored in the TSC field. Some of them designed better representations of the intersection’s observation (Han et al. 2023; Zhang et al. 2022). As a representative, FRAP (Zheng et al. 2019) utilized the spatial symmetry of intersections to improve the generalizability of the representations. Some others aggregated neighborhood information for better coordination by incorporating graph neural networks (Wei et al. 2019b; Wu et al. 2021a) or introducing *pressure* observation that accounts for the balance of the neighborhood traffic distributions. However, these works typically target small-scale scenarios and can hardly be used in large-scale scenarios due to high resource requirements (Liu et al. 2023): since they assign each intersection one independent policy network, there will be an extremely high memory demand for parameters when coming to the thousand-scale optimization. (Chen et al. 2020; Liu et al. 2023) solved this problem by introducing the parameter-sharing training paradigm, however, both of them neglected the heterogeneity of intersections and the informative neighborhood interactions to boost coordination. Moreover, their evaluations were limited to gridded road networks, possibly obscuring their shortcomings in handling heterogeneous intersections and intricate between-intersection relations that are common in real-world road networks.

Therefore, we aim to address the limitations of existing parameter-sharing methods, constructing a full parameter-sharing method that effectively models heterogeneous intersections and their intricate interactions in city-scale traffic signal control. However, this task is quite challenging. Since full parameter-sharing methods adopt one unified policy net-

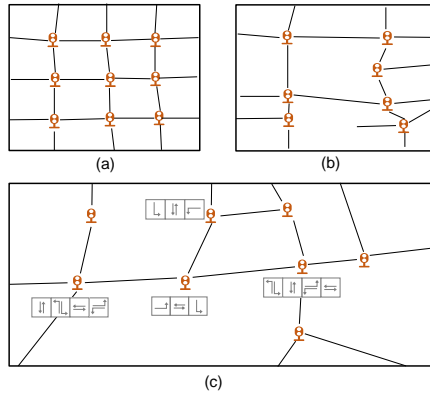


Figure 1: Illustrations of (a) gridded and evenly distributed intersections commonly seen in existing TSC benchmarks (b) heterogeneous intersections with intricate between-intersection connections in the real-world road network. (c) Due to phase disorder, combining the states of each phase results in inconsistent intersection observations, and simply aggregating observations from neighboring intersections fails to convey the impact of incoming traffic.

work for various intersections, the representations of each intersection’s partial observation should be aligned, allowing the shared policy network to learn common decision patterns. However, both the alignment of an intersection’s self-observation and its influences from the neighborhood are challenging (Fig 1(c)). For one part, due to the inherent complexity of road networks, intersections vary across the entire city in terms of configurations and scales. Developing an aligned self-observation is challenging because it requires standardizing observation terms across heterogeneous intersections with varying phase compositions and scales, while simultaneously preserving their unique characteristics. For another, the observational data from a neighboring intersection are semantically irrelevant to a target intersection unless the relative traffic relations of their traffic movements are specified. The inconsistent traffic movement order at each intersection and the varying relative positioning (direction and distance) among intersections add significant complexity to specifying these relationships. As a result, identifying a representational space that accurately aligns the semantic impact of neighboring intersections is particularly challenging.

To address the aforementioned challenges, we propose our **CityLight** model. CityLight adopts a well-acknowledged parameter-sharing training framework, MAPPO (Yu et al. 2022a) to ensure city-level scalability. To achieve the two types of alignments, CityLight features a universal representation module that aligns not only the inner state representations of heterogeneous intersections but also representations of impacts of neighborhood intersections. Specifically, the former goal is achieved by proposing a phase reindexing rule that unifies the semantics of action sets of heterogeneous intersections and designing observations that preserve the diverse configuration and scale information. After phase reindexing, the relative traffic relations are narrowed. The latter

goal is thereby met by using a relation encoder and an impact modeling module to encode the relative traffic relation and map the neighborhood representation onto a relative traffic impact space. An attentive group fusion follows to aggregate neighborhood impacts based on competitive relationships. Besides universal representation, CityLight also features a reward integration module that combines neighborhood considerations into the reward design, thereby further boosting coordination. Our contributions can be summarized into the following four points:

- We target the coordinated traffic signal control problem for city-scale heterogeneous intersections, aiming to construct a universal model that can provide a generalizable policy for various intersections with intricate neighboring situations.
- By characterizing local traffic states and relative traffic impacts from neighboring intersections in an aligned manner, CityLight achieves city-level scalability with a parameter-sharing framework while ensuring consistent applicability to heterogeneous intersections and effective coordination under complex neighborhood interactions.
- Extensive experiments on five large-scale datasets with hundreds to tens of thousands of authentic intersections have validated the effectiveness of CityLight, with an overall 11.68% improvement and a superiority of 22.59% in transfer scenarios in throughput.
- We have also open-sourced our large-scale datasets collected from the real world, which are the first to achieve city-level optimization at the scale of ten thousand intersections, thereby facilitating the advancement of city-level traffic signal control optimization.

Related Work

Recent years have witnessed a boom in the utilization of reinforcement learning to tackle traffic signal control problems. Existing methods include two main types of advancements: better representation of the intersection’s observation, and better coordination design with neighborhood intersections. One straightforward way to derive a more informative intersection representation is to improve the observation expression. (Wu et al. 2021b) improved the pressure observation (Varaiya 2013) by measuring the difference between the average queue length on entering lanes and exiting lanes instead of the sum, thereby accounting for the impact of the road scale. (Zhang et al. 2022) introduced the count of running vehicles entering the intersections to better characterize the upcoming intersection states. Another way to improve the intersection representation is to adjust the model design to characterize some intrinsic characteristics of intersections. A representative case is FRAP (Zheng et al. 2019), which designed a phase competition modeling module to achieve invariance to symmetrical cases such as flipping and rotation in traffic flow, thereby increasing generalization. Concerning better intersection coordination, some works incorporated graph neural networks to better aggregate neighborhood states (Wei et al. 2019b; Wu et al. 2021a), some adjusted the reward design to consider the traffic situations of neighborhoods (Wei et al. 2019a), while some hierarchically optimized the whole

traffic signal system (Xu et al. 2021; Ma and Wu 2023). However, these works primarily target small-scale scenarios and face some challenges to apply to large-scale TSC. While the centralized ones (Xu et al. 2021) suffer from dimension explosion problem, the other ones (Wei et al. 2019b; Wu et al. 2021a; Zheng et al. 2019) face a high demand for resources since they assign each agent one independent policy network.

With the increasing awareness of the importance of large-scale TSC, there have been some trials in incorporating group partition to decrease the scale of each group or adopting a parameter-sharing paradigm. Regarding the former type, some works partitioned the large intersection set into several groups by clustering (Gu et al. 2024; Jiang et al. 2021). However, when the scale amounts to the city level, there may be a dilemma between the number of subgroups and the scale of each subgroup, both adding to the training efforts. Some other works came up with parameter-sharing methods to decrease the demand for resources. For example, MP-Light (Chen et al. 2020) proposed a parameter-sharing DQN agent to achieve thousand-scale optimization. GPLight (Liu et al. 2023) dynamically partitioned the signals into subgroups and adopted parameter sharing within each group. However, these parameter-sharing methods neglect the alignment of the representations of heterogeneous intersections and their influences from neighborhood intersections, thereby hindering the emergence of some correlations in experiences and leading to insufficiency of their shared policy networks in finding commonly effective strategies.

To mention, although large-scale TSC has been widely explored in literature, city-scale TSC, which usually comprises thousands of intersections and more, remains underexplored. To the best of our knowledge, only MPLight (Chen et al. 2020) and GPLight (Liu et al. 2023) conducted experiments on thousands of traffic signals. However, while the Manhattan dataset used in MPLight is a relatively gridded and evenly distributed road network, the latter work also uses a synthetic gridded road network to evaluate its large-scale capability (Appendix B.1). Therefore, we may conclude that existing city-level works lack comprehensive evaluations in complex heterogeneous road networks that commonly exist in the real world, possibly obscuring their shortcomings in handling heterogeneous intersections and intricate between-intersection coordinations.

Preliminaries

Traffic signal control refers to the transition of traffic signal states at intersections. An *intersection*, as cased in Figure 2(a), connects several *roads* at their ends, where each road includes several *lanes* pointing to different *traffic movements*. A *traffic phase* is defined as valid and contradictory traffic movements at a time. Real-world intersections mainly comprise three-phase and four-phase intersections, whose corresponding phase sets are illustrated in Figure 2(a).

We formulate our reinforcement learning-based large-scale traffic signal control problem as follows: At each time step t , agent i views part of the environment, including the traffic situation, current traffic signal, and road network attributes, as its observation o_i^t . Given the traffic and road situations and current traffic signal phases, the goal of the agent is to

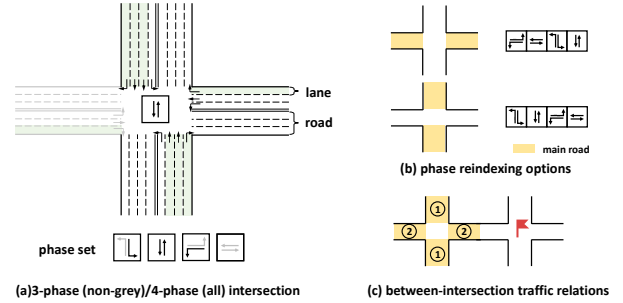


Figure 2: Illustration of (a) terms in traffic signal control problem; (b) phase reindexing operation; (c) between-intersection traffic relations. Best viewed in colors.

take an optimal action a (which phase to set) to maximize its cumulative reward r .

CityLight: A Universal Model for City-scale Real-world TSC Coordination

While parameter-sharing has been validated as effective for large-scale optimization, existing methods neglect the alignment of representations of heterogeneous intersections and how their neighborhood will exert traffic impacts on them, hindering the shared policy network from finding a universal strategy for various scenarios. To bridge the gap, we propose CityLight, whose framework is illustrated in Figure 3. CityLight features two main designs: a universal representation module and a reward integration module. In the universal representation module, we align both the observation of heterogeneous intersections, but also the traffic impact representation from neighborhoods. In the reward fusion module, we incorporate neighborhood rewards into our reward design to boost coordination.

Universal Representation

Observation Alignment for Heterogeneous Intersections Phase Reindexing. While we have defined the phase set for three-phase and four-phase intersections in the preliminary definitions, the phases have no order within the set. We introduce phase reindexing operation for two reasons: Firstly, since we use a unified policy network for all agents, reindexing phases to the uniform phase order can align phases of the same index to be of the same traffic movement semantics, thereby helping the policy network better identify the decision logics for the exact traffic movements. Secondly, the ordered phase set paves the way for convenient specifications of the relative traffic movement relations between a neighboring intersection’s phase set and the target intersection’s. As illustrated in Figure 2(b), selecting any road as the main road, the phases for a four-phase intersection can be ordered as the *left-turn phase*, *straight-through phase*, *left-turn phase in the cross-direction*, and *straight-through phase in the cross-direction*. For three-phase intersections, a T-intersection only comprises the first three phases, and a Y-intersection contains three identical phases and does not need reindexing. The reindexed phase orders are fixed thereafter. We provide case examples in Appendix A to help understand the phase reindexing operation.

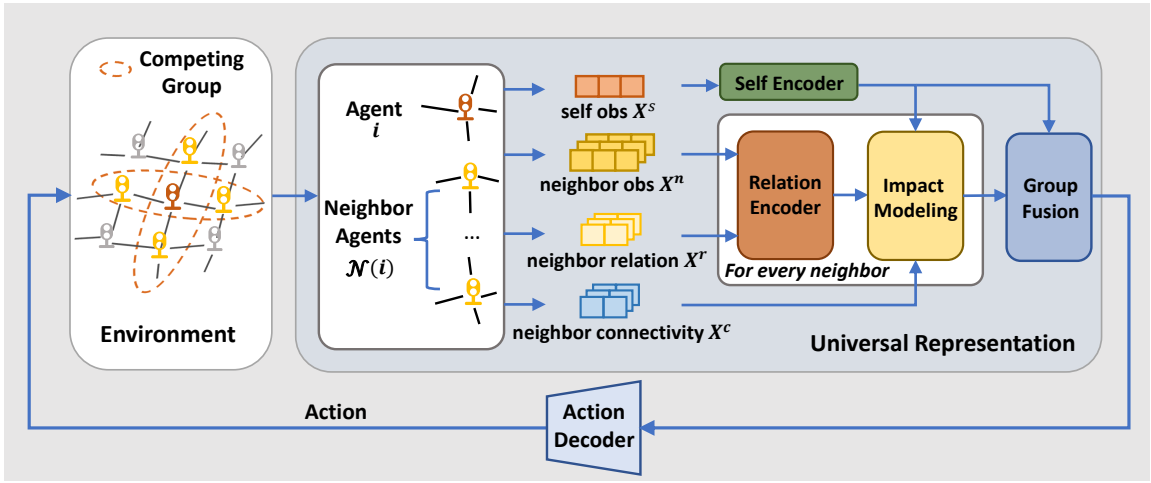


Figure 3: Overall framework of **CityLight**. CityLight features a universal representation and a reward integration module. The universal representation module achieves the alignment of observations for heterogeneous intersections, along with their impacts from neighbors that have various traffic relations to the target. Neighbor representations are further fused according to their mutual competing relations. The reward integration takes situations of the neighborhood into account in reward design for achieving better coordination.

Observation Extraction. Our observation comprises information on the traffic situation, the current phase, and the intersection heterogeneous attribute. Specifically, the observation X is concatenated from a four-digit vector representing the sum of the queuing vehicles at each phase, a four-digit one-hot action vector indicating the current passing phase, and a four-digit in-lane number vector for each phase denoting the intersection scale. For three-phase intersections, the fourth digit of each vector is padded by -1.

Neighborhood Representation Alignment for Coordination Neighborhood information has been validated informative for coordination (Wei et al. 2019b; Wu et al. 2021a). However, existing approaches that incorporate neighborhood information are typically non-parameter-sharing and assign each agent an independent policy network. Thereby, without the need for explicit specifications of the relative traffic relations from neighborhood intersections, which is information such as which phase of the neighbor will bring incoming vehicles to or accept outgoing vehicles from our target intersection, the individual policy network can implicitly learn the relations through the correlations in experiences. However, since we rely on parameter-sharing for large-scale optimization, it is necessary that we explicitly distinguish different traffic relations and align them for learning shared policy. Luckily, with phase reindexing, the scopes of relative traffic movements from a neighborhood intersection are narrowed. Therefore, we introduce the relation encoder and impact modeling module to map the neighborhood intersections’ observation onto a uniform space denoting the relative traffic impacts, and a group fusion module to attentively fuse neighborhood representations based on their mutual competing relationships.

Relation Encoder. Since the orders of phases are fixed after phase reindexing, the traffic relation from a neighboring in-

tersection to the target intersection is determined by mutual relations between their main roads, which has two possibilities as illustrated in Figure 2(c). Therefore, the relation can be encoded with a two-digit one-hot vector R , with each one representing a type of phase order regarding relative traffic movement. The process can be formulated as

$$R_{ij} = \begin{cases} [1, 0] & \text{if main roads intersect} \\ [0, 1] & \text{if main roads don't intersect} \end{cases}, j \in \mathcal{N}(i). \quad (1)$$

With the encoded traffic relation, we incorporate the cross-attention mechanism to map the initial neighborhood observation onto the relative traffic movement semantics. Specifically, with the relative relation R as the query and the original observation X of the neighboring intersection as the reference, the outputted representations by the cross-attention mechanism align, meaning that the same part in the representations corresponds to the same relative traffic movement to the target intersection. The mapped representations are further fed into the self-attention layer to extract informative parts. The process can be formulated as

$$X_j^r = \text{Self-Att}(\text{Att}(X_j, f(R_{ij}))), j \in \mathcal{N}(i). \quad (2)$$

Here f is a learnable mapping layer, X is the original observations of neighboring intersections of intersection i and R is their relation vectors, \mathcal{N} is the set of one-hop neighbors, $\text{Self-Att}(r)$ and $\text{Att}(r, q)$ are short for self-attention and attention.

Impact Modeling. Distance and linking strength (number of connected lanes) between the target intersection and a neighboring intersection, which can be summarized as their connectivity C , influence the impact intensity from neighboring intersections. Therefore, we propose our connectivity-based

impact modeling module to characterize the relative impact from the neighborhood, where the connectivity information C and the target intersection’s observational representation are used as the query in the cross-attention mechanism to model the intensity of the relative impact from neighboring interactions. To extract the informative part, we exert a self-attention mechanism on the target intersection’s original observation to generate the observation representation of the target intersection. The whole process can be formulated as

$$X_j^n = \text{Att}(X_j^r, \text{Self} - \text{att}(X_i) || f(C_{ij})), j \in \mathcal{N}(I). \quad (3)$$

Here f is a learnable mapping layer and $||$ denotes vector concatenation.

Group Fusion. Due to the flipping symmetry of intersections, the impact of flipped neighbors on the target intersection is homogeneous and the two groups of flipped neighbors are typically orthogonally laid out with competitive impacts on the target intersection’s signal choice. Thereby, we denote each group of flipped neighbors as **competing group** (as cased in Figure 3). We order the competing group along the main road as the first and the one along the crossed road as the second and attentively aggregate neighboring representations from a group by putting higher weight on noteworthy neighboring patterns. Specifically, for neighboring intersection j in the m -th competing group \mathcal{N}_{c_m} of intersection i , the importance weights are calculated by

$$a_j = c \cdot \text{Tanh}(W \cdot X_j^n + b), j \in \mathcal{N}_{c_m}(I), m \in \{0, 1\}, \quad (4)$$

$$s_j = \frac{e^{a_j}}{\sum_{k \in \mathcal{N}_{c_m}(i)} e^{a_k}}, j \in \mathcal{N}_{c_m}(i), m \in \{0, 1\}. \quad (5)$$

Here $W \in \mathbb{R}^{1 \times d}$, $b \in \mathbb{R}^1$, and $c \in \mathbb{R}^1$ are the learnable parameters, and d is the dimension of neighboring representations $\{X^n\}$. The final overall representation of the target intersection i is

$$X_i^f = \text{Self} - \text{Att}(X_i) || \sum_{j \in \mathcal{N}_{c_1}(i)} s_j X_j^n || \sum_{j \in \mathcal{N}_{c_2}(i)} s_j X_j^n, \quad (6)$$

where X^n is calculated from Equ 3. Based on the representations, a multi-layer perception with the softmax layer outputs the selection possibilities of the action set, which are the reindexed phases.

Reward Integration

Existing literature in traffic signal controls typically assigns independent rewards for intersections, aiming to maximize each intersection’s traffic efficiency. However, the combination of local optimal policies does not ensure a global optimal policy (Xu et al. 2021). Releasing numerous vehicles from one upstream intersection to the already congested downstream intersection might enhance the traffic efficiency itself, but it could exacerbate extreme congestion at the downstream

intersection, even leading to a gridlock. Thus, it is important to integrate neighboring intersections’ situations into the optimization target. Specifically, we combine the original rewards of neighboring intersections with the intersection’s own original reward. To dismiss the impact of imbalanced numbers of neighbors, the rewards of one-hop neighbors are averaged before being added to the target intersection’s reward, and the two terms are balanced with a tunable coefficient. In our implementation, we choose the well-acknowledged average queue length metric as the original reward (Wei et al. 2019b; Zheng et al. 2019; Zang et al. 2020). The integrated reward can be formulated as

$$r_i^f = r_i + \alpha \cdot \frac{\sum_{j \in \mathcal{N}(i)} r_j}{|\mathcal{N}(i)|}, \quad (7)$$

where r denotes the original independent rewards, $\mathcal{N}(i)$ denotes the one-hop neighbor set of intersection i , $|\mathcal{N}(i)|$ denotes the number of one-hop neighbors, and α is a tunable balancing coefficient to balance between local optimal and neighborhood optimal.

Numerical Experiments

Experimental Setup

This section summarizes the setting of our testbed, datasets, baselines, and metrics. More details are in Appendix C.

Testbed. We conduct experiments on MOSS (Zhang et al. 2024) simulator¹. Adopting GPU acceleration, MOSS significantly improves the efficiency and scale of traffic simulation, thereby enabling realistic and fast simulations for large-scale road networks (Zhang et al. 2024). The experimental setting of the TSC follows existing works (Wu et al. 2023): for every 15-second time interval, each model assigns each intersection what it considers the optimal traffic phase. The optimization scenario involves traffic flow in the morning rush within a 60-minute timeframe.

Datasets. For comprehensive evaluations, we adopt one benchmark dataset, **Manhattan (196 intersections)**, and construct another four high-authenticity datasets, including two region-scale datasets with hundreds of intersections, **Chaoyang (97 intersections)** and **Central Beijing (885 intersections)**, and two city-scale datasets with thousands and even tens of thousands of intersections, **Jinan (3930 intersections)** and **Beijing (13952 intersections)**. The vehicle trajectories of our constructed datasets closely replicate real-world traffic demands: For datasets of Beijing, the vehicle trajectories are generated based on the true hour-level OD flow matrix collected from a Chinese location-based service (LBS) provider in 2020. For Jinan, the vehicle trajectories are recovered from traffic camera videos (Yu et al. 2023, 2022b).

Baselines and Metrics. Our baselines comprise three rule-based methods, seven RL-based methods, and one large language model-empowered TSC method. For rule-based methods, we include Fixed Time (Koonce et al. 2008) and Max

¹<https://moss.fiblab.net/>

Table 1: Average performances on three random seeds in three region-scale and two city-scale datasets. Bold denotes the best results and underline denotes the second-best. '-' denotes 'no result' due to extremely high resource demands or expenses. The standard deviations of the results are provided in Appendix C. TP and ATT are short for throughput and average travel time.

Model	Manhattan		Chaoyang		Central Beijing		Jinan		Beijing	
	TP↑	ATT↓	TP↑	ATT↓	TP↑	ATT↓	TP↑	ATT↓	TP↑	ATT↓
Fixed Time	2343	1687.5	6076	826.7	18602	1514.9	33681	1605.2	60615	1133.5
Max Pressure	2731	1587.8	1215	1776.1	5448	1879.9	2492	2051.7	15563	1566.7
Adjusted Max Pressure	3371	1499.1	5909	785.3	<u>18950</u>	<u>1497.4</u>	33367	<u>1601.8</u>	64613	1090.3
FRAP	1957	1682.1	6188	920.1	17156	1575.8	—	—	—	—
CoLight	3480	1519.3	6661	758.2	18584	1490.8	—	—	—	—
MPLight	3136	1574.7	6104	888.2	17535	1550.4	30476	1633	60652	1145.9
Efficient-MPLight	2819	1636.0	5916	964.6	16063	1592.3	29249	1659.4	57826	1164.6
Advanced-CoLight	<u>3523</u>	<u>1514.9</u>	<u>6730</u>	<u>749.3</u>	17608	1548.3	—	—	—	—
Advanced-MPLight	3339	1547.9	6347	814.3	16691	1578.2	<u>33800</u>	1608.7	<u>64764</u>	<u>1088.2</u>
GPLight	3091	1588.6	5892	949.1	17499	1580.8	29899	1660.1	60250	1149.8
LLMLight	2325	1716.7	1835	1653.6	7568	1828.2	—	—	—	—
CityLight (Ours)	3962	1422.9	7702	599.5	21548	1437.9	36742	1553.6	70451	1030.1
Improvement	12.46%	6.07%	14.45%	23.65%	13.71%	3.97%	8.70%	3.01%	9.05%	5.34%

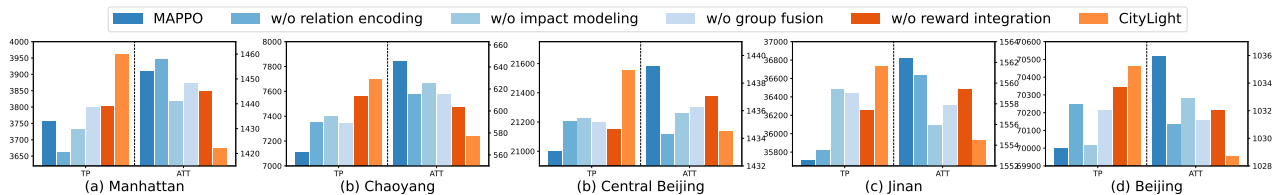


Figure 4: Performance of ablation variants.

Pressure (Varaiya 2013), and Adjusted Max Pressure. For RL-based methods, we include FRAP (Zheng et al. 2019), CoLight (Wei et al. 2019b), MPLight (Chen et al. 2020), Efficient-MPLight (Wu et al. 2021b), Advanced-CoLight (Zhang et al. 2022), Advanced-MPLight (Zhang et al. 2022), and GPLight (Liu et al. 2023). The advanced generalization capabilities of LLMs have spurred their application in TSC (Lai et al. 2023; Feng et al. 2024). Therefore, we also compared with LLMLight (Lai et al. 2023) with GPT-4o-mini as the agent. We use two widely adopted evaluation metrics indicating the overall traffic efficiency: throughput (TP), and average travel time (ATT).

Overall Performance

We compare CityLight with baselines in three region-scale datasets and two city-scale datasets as shown in Table 1. FRAP, Colight, and Advanced-Colight are non-parameter-sharing methods that assign each intersection an independent policy network, thereby they require an excessively high memory demand which makes them unsuitable for large-scale scenarios. LLMLight, which is empowered by large language models, also suffers from unbearable API expenses in large-scale scenarios. Therefore, we only list their performance on region-scale datasets. Based on Table 1, we have these noteworthy observations:

- **Consistent Superiority.** Our CityLight consistently achieves the best performance across different metrics and datasets. For region-level experiments, our method outperforms all state-of-the-art baselines, with an average lift of 13.54% in terms of throughput and an average reduction

of 11.23% in terms of average travel time. When evaluated at the city level, our method also shows an astonishing improvement of 8.88% in throughput and 4.18% in average travel time. The significant performance gain demonstrates CityLight’s effectiveness in achieving coordinated TSC for intricate real-world traffic and road networks.

- **Incapability of existing large-scale TSC methods to achieve coordination among heterogeneous intersections.** When scaled to the city level, the performances of MPLight, Efficient-MPLight, Advanced-MPLight, and GPLight may even perform worse than rule-based methods. The reason may be their insufficiency in aligning the observation semantics of each intersection and representations of the neighborhood impacts, thereby hindering the shared policy network from learning a universally applicable and more effective strategy.

Ablation Studies

CityLight proposes several important designs to make the universal policy learned by MAPPO applicable to heterogeneous and intricate real-world intersections: relation encoder, impact modeling, group fusion for universal representation, and reward integration. As shown in Figure 4, removing relation encoding decreases the performance by 2.23% in throughput, indicating the importance of mapping neighborhood representations onto a uniform semantic space that denotes relative traffic movements. Removing impact modeling causes a decrease of 1.66%, strengthening the importance of explicitly modeling the impact of distance and connection intensity. Meanwhile, removing group fusion will also lead

Table 2: Generalizability of CityLight and baselines across scale and city. Bold denotes the best results and underline denotes the second-best ones. Due to space limits, we shorten Chaoyang to 'CY' and Central Beijing to 'CB'.

Model	CB->CY		CY->CB		Beijing->Jinan		Jinan->Beijing	
	TP↑	ATT↓	TP↑	ATT↓	TP↑	ATT↓	TP↑	ATT↓
MPLight	5048	1025.9	15010	1624.6	26621	1695.3	52615	1185.7
Efficient-MPLight	1955	1626.1	14966	1625.8	23144	1748.7	53175	1207.8
Advanced-MPLight	<u>5137</u>	<u>926.2</u>	<u>15040</u>	<u>1623.3</u>	<u>29933</u>	<u>1635.8</u>	<u>57199</u>	<u>1150.3</u>
CityLight (Ours)	6704	741.5	19648	1476.5	34016	1579.8	66116	1070.5
Improvement	30.50%	19.94%	30.64%	9.04%	13.64%	3.42%	15.59%	6.94%

Table 3: Performance comparisons of full parameter sharing across different configurations against separate parameter sharing for each configuration group in terms of throughput. Here 'CB' is short for Central Beijing for page limit.

	Chaoyang	CB	Jinan	Beijing
Separate	7325	20944	35943	70031
Unified	7702	21548	36742	70451
Improv.	5.15%	2.88%	2.22%	0.60%

to a 1.85% decrease. This indicates the effectiveness of our attentive group fusion module in integrating and differentiating information from neighbors with varying competitive relationships. Last but not least, our reward integration design also brings a 1.28% performance gain of throughput, showing its contribution to boosting coordination.

Generalizability Test

We conduct generalizability tests on our CityLight and parameter-sharing baselines by testing their direct transfer performances. We select two transfer pairs: The first pair is Chaoyang and Central Beijing for evaluations of generalizability across scales. The second pair is Beijing and Jinan for evaluations of generalizability across cities. As in Table 2, CityLight shows great transferability across both scale and city. Compared with the non-transfer scenarios, the performance gain of CityLight over the best baseline enlarges, with an average improvement of 30.57% when transferred across scales and 14.62% when transferred across cities in terms of throughput. Moreover, while parameter-sharing learning-based baselines all show a worse performance compared with the best rule-based method (Table 1), our CityLight outperforms rule-based methods. All these statistics validate the excellent generalizability of our CityLight which derives from learning from the universal representations of heterogeneous intersections with various neighborhood interactions.

Effectiveness of Full Parameter Sharing Across the Entire City

In our CityLight, we propose the universal representation module to represent intersections with heterogeneous configurations in an aligned manner and adopt full parameter sharing to learn a universal policy. Here we present the effectiveness of such full parameter sharing across configuration and space.

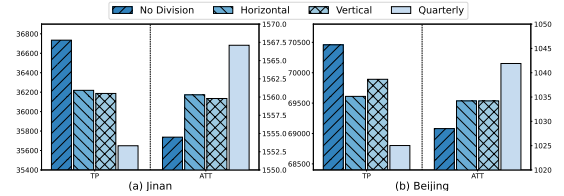


Figure 5: Performance of full parameter sharing against parameter sharing in subgroups divided horizontally, vertically, and quarterly.

Effectiveness of full parameter sharing across heterogeneous intersections. As shown in Table 3, with aligned representations, adopting full parameter sharing outperforms separate parameter sharing for heterogeneous intersections, bringing an average performance gain of 2.71% in terms of throughput. It therefore validates the effectiveness of the universal representation module in aligning representations of different configurations from the uniform traffic movement semantics to learn shared decision logic while preserving their heterogeneity.

Effectiveness of full parameter sharing across space. Although conducting city-level traffic signal control is essential, it remains a question whether intersections across space fit into a unified traffic signal control strategy. Thereby, we conducted a case study of CityLight in Jinan and Beijing where we divided the dataset into halves horizontally, vertically, and into quarters and adopted parameter-sharing in each subgroup. As shown in Figure 5, as the number of sub-regions increases, the performance of the overall city traffic signal control system declines. This phenomenon implies that agents in traffic signal control share a common target, thereby full parameter sharing is effective, and the increase of shared agents and experiences improves the effectiveness and generalizability of our learned policy.

Conclusion

In this work, we propose CityLight to achieve coordinated traffic signal control for city-scale heterogeneous intersections. Featuring a universal representation module that aligns not only the observation semantics of heterogeneous intersections but their intricate impacts on neighborhood intersections, and a reward integration module to integrate neighborhood rewards for better coordination, the parameter-sharing learning manages to learn a universally applicable TSC control strategy. The great performance gain on five datasets

that scale to the ten thousand level validates the effectiveness of CityLight. The following transfer tests and analyses further strengthen the generalizability of CityLight, proving its potential to be applied in diverse urban environments and boosting overall traffic efficiency.

References

- Afrin, T.; and Yodo, N. 2020. A survey of road traffic congestion measures towards a sustainable and resilient transportation system. *Sustainability*, 12(11): 4660.
- Chen, C.; Wei, H.; Xu, N.; Zheng, G.; Yang, M.; Xiong, Y.; Xu, K.; and Li, Z. 2020. Toward a thousand lights: Decentralized deep reinforcement learning for large-scale traffic signal control. In *Proceedings of the AAAI conference on artificial intelligence*, volume 34, 3414–3421.
- Chien, S. I.; Kim, K.; and Daniel, J. 2006. Cost and Benefit analysis for optimized signal timing-case study: New Jersey route 23. *Institute of Transportation Engineers. ITE Journal*, 76(10): 37.
- Feng, J.; Zhang, J.; Yan, J.; Zhang, X.; Ouyang, T.; Liu, T.; Du, Y.; Guo, S.; and Li, Y. 2024. CityBench: Evaluating the Capabilities of Large Language Model as World Model. *arXiv preprint arXiv:2406.13945*.
- Feng, S.; Yan, X.; Sun, H.; Feng, Y.; and Liu, H. X. 2021. Intelligent driving intelligence test for autonomous vehicles with naturalistic and adversarial environment. *Nature communications*, 12(1): 748.
- Gu, H.; Wang, S.; Ma, X.; Jia, D.; Mao, G.; Lim, E. G.; and Wong, C. P. R. 2024. Large-scale traffic signal control using constrained network partition and adaptive deep reinforcement learning. *IEEE Transactions on Intelligent Transportation Systems*.
- Han, X.; Zhao, X.; Zhang, L.; and Wang, W. 2023. Mitigating action hysteresis in traffic signal control with traffic predictive reinforcement learning. In *Proceedings of the 29th ACM SIGKDD Conference on Knowledge Discovery and Data Mining*, 673–684.
- Jiang, Q.; Qin, M.; Shi, S.; Sun, W.; and Zheng, B. 2022. Multi-agent reinforcement learning for traffic signal control through universal communication method. *arXiv preprint arXiv:2204.12190*.
- Jiang, S.; Huang, Y.; Jafari, M.; and Jalayer, M. 2021. A distributed multi-agent reinforcement learning with graph decomposition approach for large-scale adaptive traffic signal control. *IEEE Transactions on Intelligent Transportation Systems*, 23(9): 14689–14701.
- Kesting, A.; Treiber, M.; and Helbing, D. 2007. General lane-changing model MOBIL for car-following models. *Transportation Research Record*, 1999(1): 86–94.
- Koonce, P.; et al. 2008. Traffic signal timing manual. Technical report, United States. Federal Highway Administration.
- Lai, S.; Xu, Z.; Zhang, W.; Liu, H.; and Xiong, H. 2023. Large language models as traffic signal control agents: Capacity and opportunity. *arXiv preprint arXiv:2312.16044*.
- Liu, Y.; Luo, G.; Yuan, Q.; Li, J.; Jin, L.; Chen, B.; and Pan, R. 2023. Gplight: grouped multi-agent reinforcement learning for large-scale traffic signal control. In *Proceedings of the Thirty-Second International Joint Conference on Artificial Intelligence*, 199–207.
- Ma, J.; and Wu, F. 2023. Learning to Coordinate Traffic Signals With Adaptive Network Partition. *IEEE Transactions on Intelligent Transportation Systems*.
- Treiber, M.; Hennecke, A.; and Helbing, D. 2000. Congested traffic states in empirical observations and microscopic simulations. *Physical review E*, 62(2): 1805.
- Varaiya, P. 2013. The max-pressure controller for arbitrary networks of signalized intersections. In *Advances in dynamic network modeling in complex transportation systems*, 27–66. Springer.
- Wei, H.; Chen, C.; Zheng, G.; Wu, K.; Gayah, V.; Xu, K.; and Li, Z. 2019a. Presslight: Learning max pressure control to coordinate traffic signals in arterial network. In *Proceedings of the 25th ACM SIGKDD international conference on knowledge discovery & data mining*, 1290–1298.
- Wei, H.; Xu, N.; Zhang, H.; Zheng, G.; Zang, X.; Chen, C.; Zhang, W.; Zhu, Y.; Xu, K.; and Li, Z. 2019b. Colight: Learning network-level cooperation for traffic signal control. In *Proceedings of the 28th ACM international conference on information and knowledge management*, 1913–1922.
- Wu, L.; Wang, M.; Wu, D.; and Wu, J. 2021a. Dynstgat: Dynamic spatial-temporal graph attention network for traffic signal control. In *Proceedings of the 30th ACM international conference on information & knowledge management*, 2150–2159.
- Wu, Q.; Li, M.; Shen, J.; Lü, L.; Du, B.; and Zhang, K. 2023. Transformerlight: A novel sequence modeling based traffic signaling mechanism via gated transformer. In *Proceedings of the 29th ACM SIGKDD Conference on Knowledge Discovery and Data Mining*, 2639–2647.
- Wu, Q.; Zhang, L.; Shen, J.; Lü, L.; Du, B.; and Wu, J. 2021b. Efficient pressure: Improving efficiency for signalized intersections. *arXiv preprint arXiv:2112.02336*.
- Xu, B.; Wang, Y.; Wang, Z.; Jia, H.; and Lu, Z. 2021. Hierarchically and cooperatively learning traffic signal control. In *Proceedings of the AAAI conference on artificial intelligence*, volume 35, 669–677.
- Yu, C.; Velu, A.; Vinitzky, E.; Gao, J.; Wang, Y.; Bayen, A.; and Wu, Y. 2022a. The surprising effectiveness of ppo in cooperative multi-agent games. *Advances in Neural Information Processing Systems*, 35: 24611–24624.
- Yu, F.; Ao, W.; Yan, H.; Zhang, G.; Wu, W.; and Li, Y. 2022b. Spatio-temporal vehicle trajectory recovery on road network based on traffic camera video data. In *Proceedings of the 28th ACM SIGKDD Conference on Knowledge Discovery and Data Mining*, 4413–4421.
- Yu, F.; Yan, H.; Chen, R.; Zhang, G.; Liu, Y.; Chen, M.; and Li, Y. 2023. City-scale vehicle trajectory data from traffic camera videos. *Scientific data*, 10(1): 711.
- Zang, X.; Yao, H.; Zheng, G.; Xu, N.; Xu, K.; and Li, Z. 2020. Metalight: Value-based meta-reinforcement learning for traffic signal control. In *Proceedings of the AAAI conference on artificial intelligence*, volume 34, 1153–1160.

Zhang, J.; Ao, W.; Yan, J.; Rong, C.; Jin, D.; Wu, W.; and Li, Y. 2024. MOSS: A Large-scale Open Microscopic Traffic Simulation System. arXiv:2405.12520.

Zhang, L.; Wu, Q.; Shen, J.; Lü, L.; Du, B.; and Wu, J. 2022. Expression might be enough: representing pressure and demand for reinforcement learning based traffic signal control. In *International Conference on Machine Learning*, 26645–26654. PMLR.

Zheng, G.; Xiong, Y.; Zang, X.; Feng, J.; Wei, H.; Zhang, H.; Li, Y.; Xu, K.; and Li, Z. 2019. Learning phase competition for traffic signal control. In *Proceedings of the 28th ACM international conference on information and knowledge management*, 1963–1972.

A. Phase Reindexing Illustrations

The phase indexing process consists of the following two steps: selecting one straight road in the intersection as the main road; rearranging the phases as *left-turn phase*, *straight-through phase*, *left-turn phase in the cross-direction*, and *straight-through phase in the cross-direction*. For a 4-phase intersection, since there are two options for the main road, there are two possible reindexed phase sets. For 3-phase T intersections, the main road has only one choice. For the 3-phase Y intersection, its phases are identical and reindexing-free. In this way, we set rules for the phase reindexing process for all common intersections in the real world. Moreover, the phases of the same order index correspond to generally consistent traffic movements, thereby helping the policy network better identify the decision logics for the exact traffic movements. We provide comprehensive illustrations in Fig. 6.

B. Data Descriptions

B.1 Over-Standardized Road Networks in Existing Benchmarks

Here we summarize the benchmarks commonly used to evaluate existing traffic signal control methods:

- **Hangzhou.** A grid road network with 4×4 intersections in Gudang Sub-district of Hangzhou, China. Used in (Liu et al. 2023; Jiang et al. 2022; Ma and Wu 2023; Lai et al. 2023; Wu et al. 2023; Wei et al. 2019b; Wu et al. 2021b; Xu et al. 2021; Zheng et al. 2019; Zhang et al. 2022), etc.
- **Jinan.** A grid road network with 3×4 intersections in Dongfeng Sub-district of Jinan, China. Used in (Liu et al. 2023; Jiang et al. 2022; Ma and Wu 2023; Lai et al. 2023; Wu et al. 2023; Wei et al. 2019b; Wu et al. 2021b; Xu et al. 2021; Zheng et al. 2019; Zhang et al. 2022), etc.
- **Manhattan a.** A grid road network with 196 intersections collected in Manhattan, New York, the United States. Used in (Liu et al. 2023; Jiang et al. 2022; Wu et al. 2023; Wei et al. 2019b; Xu et al. 2021; Zhang et al. 2022), etc.

And two large-scale road network benchmarks to evaluate large-scale traffic signal control methods:

- **Synthetic Grids.** A synthetic grid benchmark with 1089 intersections for large-scale TSC evaluation. Used in (Liu et al. 2023).
- **Manhattan b.** A relatively gridded road network with 2510 intersections. This benchmark was also collected in Manhattan, New York, the United States. Used in (Chen et al. 2020).

As shown in Fig. 7, these commonly used road network benchmarks are quite regularly laid out: the road networks are gridded connected, the intersections are rather homogeneous without configuration differences, and the distances between intersections are relatively uniform. However, due to the variances in road density and structure across cities, real-world road networks may exhibit more complexity. Due to constraints imposed by terrain, rivers, and existing buildings on the road, the roads may be irregularly arranged and intricately intertwined. Meanwhile, there are differences in the importance of urban roads, leading to differences in

road classes and scales. **Therefore, evaluations done on these benchmarks may not truly validate the proposed method’s consistently superior performance when facing heterogeneous intersections and complex intersection connectivity patterns.** To develop city-scale traffic signal control, it is essential to eliminate the gap between the benchmark and the intricate road network in real life.

B.2 High-authenticity Datasets Used in Our Evaluations

In our evaluations, we include one benchmark dataset, Manhattan a, and another four high-authenticity road network datasets collected from the real world. The overall statistics of the four datasets are summarized in Table 4:

- **Chaoyang** This dataset is collected in the Chaoyang district of Beijing, with a boundary of [(116.39, 39.97), (116.42, 39.97), (116.42, 40.01), (116.39, 40.01)]. The traffic signal distribution is visualized in Fig. 8a.
- **Central Beijing.** This dataset is collected at the center of Beijing, mainly covering the Dongcheng district and the Xicheng district. The region boundary is [(116.35, 39.87), (116.42, 39.87), (116.42, 39.94), (116.35, 39.94)]. and the corresponding traffic signal distribution is visualized in Fig. 8b.
- **Jinan.** A city-level dataset covering the urban areas of Jinan, with a boundary of [(116.84, 36.57), (117.35, 36.57), (117.35, 36.76), (116.84, 36.76)]. We snapshotted its intersection distribution in Fig. 9a.
- **Beijing.** A city-level dataset covering almost all urban areas of Beijing (within the sixth ring of Beijing). The boundary is [(116.14, 39.76), (116.65, 39.76), (116.65, 40.15), (116.14, 40.15)]. We snapshotted its intersection distribution in Fig. 9b.

The road network data of all four datasets is directly crawled from OpenStreetMap², a crowd-sourcing high-coverage map service website. The traffic trajectories are recovered from true OD or trajectory data to replicate real-world traffic patterns. Specifically, the traffic trajectory data in Jinan is recovered from collected junction camera data following (Yu et al. 2022b, 2023). For Beijing, traffic flows are generated from the true second-level road network-level OD matrix collected by a large Chinese location-based service (LBS) provider in 2020. All datasets include vehicles traveling during the morning rush hour from 7 to 8 am. The visualizations of the OD distribution of our datasets are presented in Fig. 10.

C. Experiments

C.1 Simulation Environment: MOSS

In this work, all experiments, including CityLight and all baselines, are consistently conducted with the traffic simulator MOSS, which is short for MObility Simulation System³. The comprehensive introduction of MOSS can be referred to in (Zhang et al. 2024). The car-following model in MOSS

²<https://www.openstreetmap.org/>

³<https://moss.fiblab.net/>

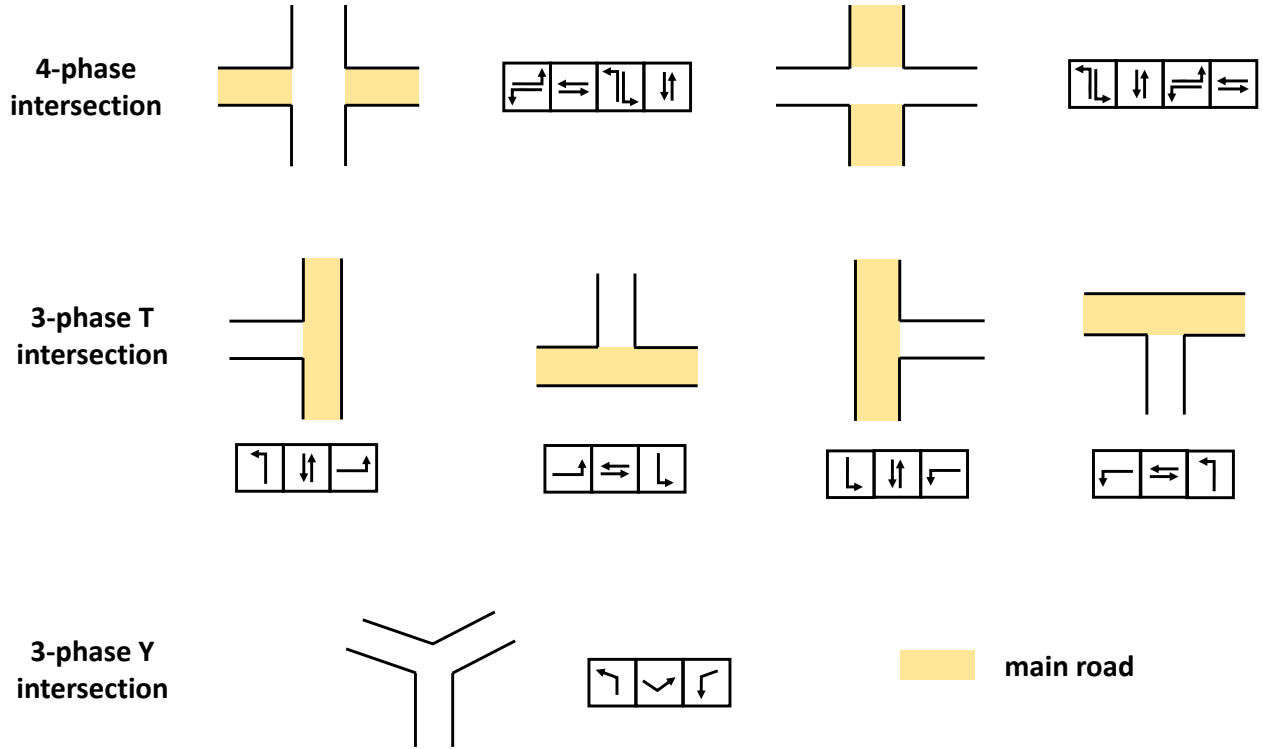


Figure 6: Illustrations of the phase reindexing operations.

Datasets	Chaoyang	Central Beijing	Beijing	Jinan
#Intersections	97	885	13952	4064
#Three-phase intersections	49	630	9752	2466
#Four-phase intersections	48	255	4200	1595
#Roads	608	4640	76806	23950
Covered Area	14.2 km^2	79.3 km^2	3104.4 km^2	1477.5 km^2
#Agents	9000	55429	143298	99712

Table 4: The basic information and statistics of four high-authenticity datasets.

is the IDM model (Treiber, Hennecke, and Helbing 2000) and the lane-changing model is a MOBIL model (Kesting, Treiber, and Helbing 2007; Feng et al. 2021). While existing microscopic simulators, such as SUMO, CityFlow, and CBLab, are typically implemented on CPUs and suffer from computational inefficiency, MOSS adopts graphics processing units (GPUs) as the main computational hardware and parallelizes all simulation computation processes to accelerate without damage to realism. On the same computational resources, a simulation of traffic involving 2.4 million vehicles over an hour reveals that MOSS can achieve a speed enhancement of 100 times compared to CityFlow, the fastest microscopic traffic simulator (Zhang et al. 2024). Meanwhile, MOSS can achieve a higher degree of realism compared with existing simulators (Zhang et al. 2024). In conclusion, the high computational efficiency and high fidelity of MOSS can ensure the fast and accurate simulation of city-scale traffic and is thereby adopted in our implementation of CityLight.

C.2 Baselines

- **Fixed Time (Koonce et al. 2008).** Transit along the phase set with the fixed time interval.
- **Max Pressure (Varaiya 2013).** Pressure is defined as the discrepancy in the number of vehicles for the entering lanes and existing lanes of a phase. Max pressure transits the traffic signal to the phase with the maximum value of pressure. In this way, the traffic system reaches equitable traffic flow.
- **Adjusted Max Pressure (Varaiya 2013).** The length of roads in real-world road systems varies a lot, leading to wide-range vehicle capacity. The initial definition of pressure overlooks the heterogeneity of vehicle capacity that causes fundamental imbalances in roads' vehicle numbers. Therefore, longer roads may be consistently experiencing high pressure and green phase, leading to vehicles on other roads being trapped. We distill such impact by redefining

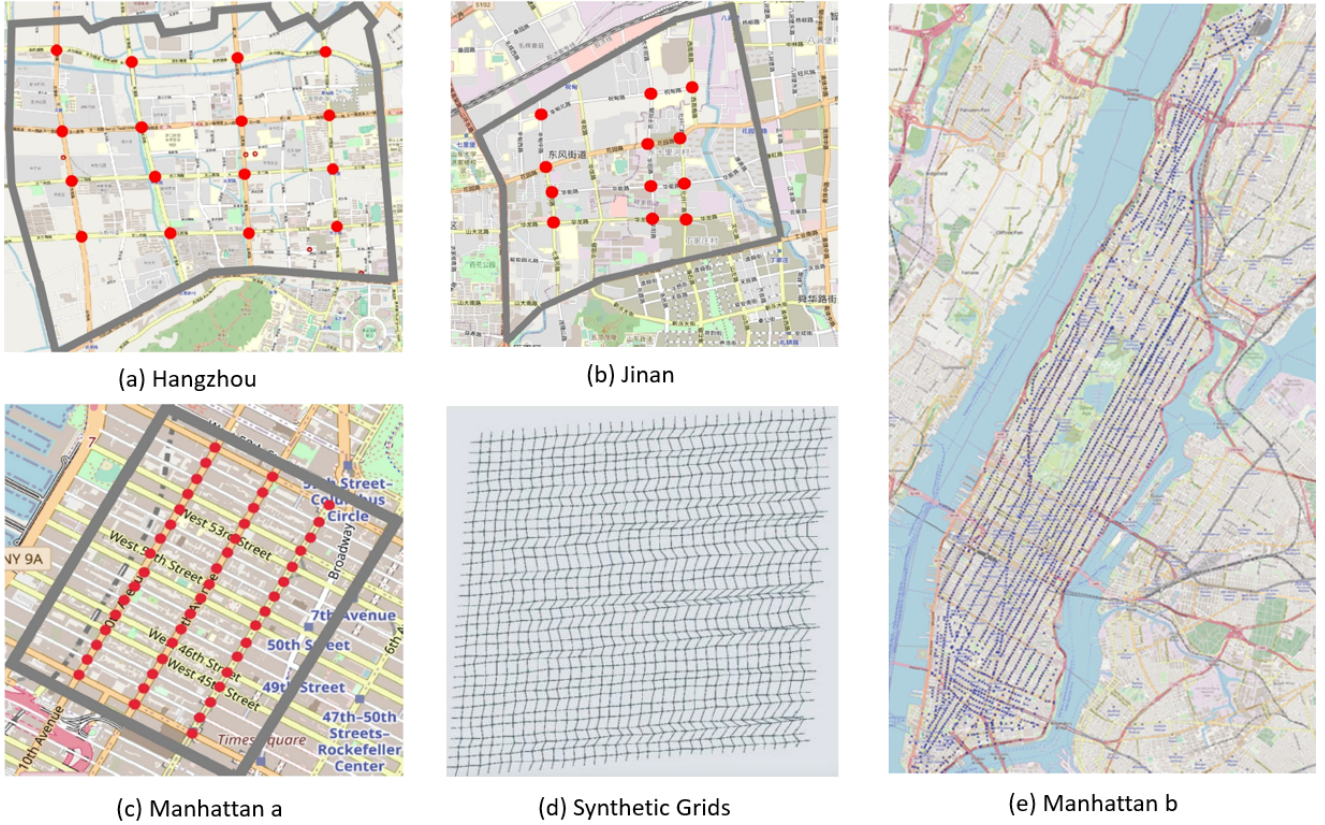


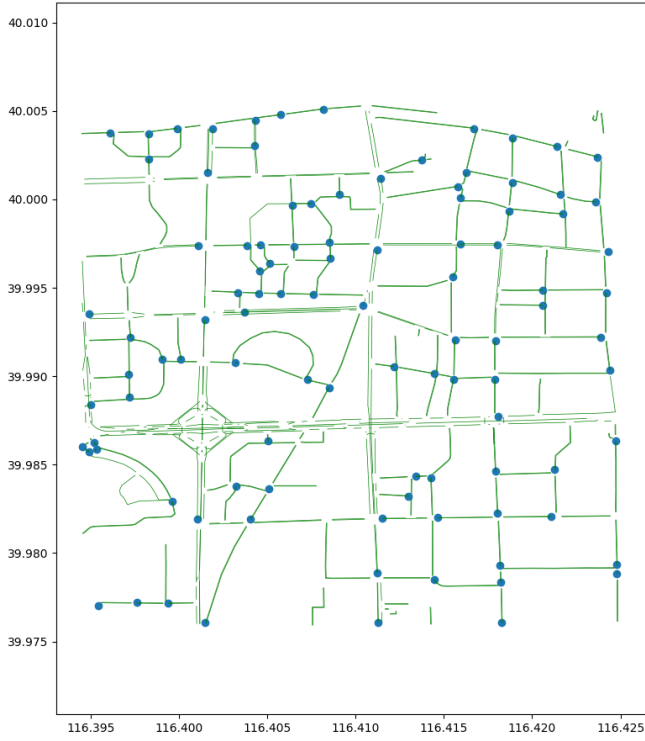
Figure 7: Benchmarks commonly used in evaluations of existing TSC works.

Parameter	Manhattan	Chaoyang	Central Beijing	Jinan	Beijing
buffer episode size	120	60	12	12	4
num mini batch	12	6	4	18	18
ppo epoch	16	16	16	10	10
balancing coefficient α	0.2	0.2	0.2	0.2	0.2

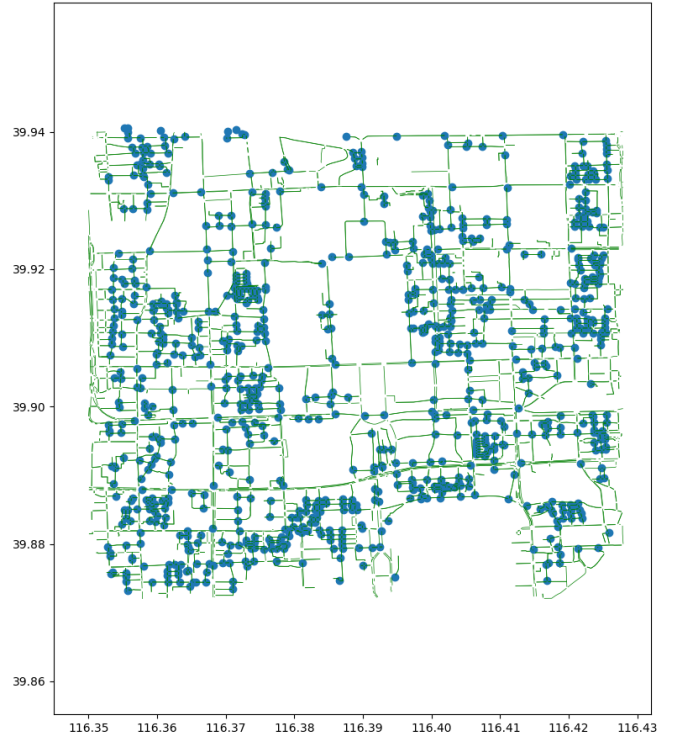
Table 5: Hyperparameters of our CityLight model on all datasets.

- pressure as the discrepancy in the number of vehicles per road length for the entering lanes and exiting lanes.
- **FRAP (Zheng et al. 2019)**. A reinforcement learning-based traffic signal control method that considers the rotation-symmetry of intersections by modeling from the perspective of phase competition relation. Each intersection has an independent policy network to be optimized.
 - **MPLight (Chen et al. 2020)**. A reinforcement learning-based method that adopts a parameter-sharing FRAP model as the unified policy network and introduces pressure of the intersection, which is the discrepancy in the number of vehicles for all entering lanes and all exiting lanes, as the reward.
 - **CoLight (Wei et al. 2019b)**. A reinforcement learning-based method that uses a graph attentional network to incorporate neighboring situations for decision. Each intersection has an independent policy network to be optimized.

- **Efficient-MPLight (Wu et al. 2021b)**. It introduces the efficient pressure into the observation space, which is calculated by the discrepancy in the number of vehicles per entering lane and per exiting lane of every phase.
- **Advanced-MPLight (Zhang et al. 2022)**. It adjusts MPLight by taking into account the running vehicles approaching the intersection in the observation.
- **Advanced-CoLight (Zhang et al. 2022)**. Built on CoLight with the same adjustment in Advanced-MPLight.
- **GPLight (Liu et al. 2023)**. A MARL method that dynamically groups intersections and shares parameters within groups.
- **LLMLight (Lai et al. 2023)**. It employs Large Language Models (LLMs) as decision-making agents for TSC. In our experiments, we use GPT-4o-mini as our agents.



(a) Chaoyang



(b) Central Beijing

Figure 8: Visualizations of intersection distribution and road networks.

C.3 Metrics

- **Throughput.** The total number of finished travels in the simulation episode. A higher throughput corresponds to a higher traffic efficiency.
- **Average Travel Time.** The average travel time spent by all vehicles in the simulation episode. A low average travel time corresponds to a higher traffic efficiency.

C.4 Implementation

Table 5 shows the best parameters of CityLight on different datasets. During the training process, we used the Adam optimizer for gradient-based model optimization. The learning rate of both the actor and the critic is set as $5e-4$ following the default setting of MAPPO (Yu et al. 2022a). Without specification, the hyperparameters follow the default setting of MAPPO (Yu et al. 2022a) as well. Generally, as the number of agents increases, the buffer episode size can be accordingly decreased as long as the overall sample size in the buffer is ensured. Num of mini size is set to split the buffer into separate batches to relieve the cost of GPU memory. Thereby, it should be set according to the available training resources. PPO epoch corresponds to the number of usage times of every training data. The PPO epoch should be set smaller in difficult environments to prevent overfitting. For the balancing coefficient α defined in the reward integration module, we grid search it in the set of $\{0.1, 0.2, 0.3\}$. For our baselines, we also finetuned their hyperparameters in each

dataset respectively for fair comparisons.

C.5 Full Experiment Tables

To fully compare CityLight with baselines, we perform experiments on CityLight and every baseline on three random seeds. Table 6 and Table 7 show the mean and standard deviation values of each method. From the tables, we can conclude that our CityLight has a consistent and significant superiority over all state-of-the-art baselines across all five datasets.

C.6 Training Curves

We visualized the training curve of both our CityLight and the state-of-the-art baselines in Fig. 11. From the figure, we can see that all of the methods reach convergence. Parameter-sharing methods have a quicker convergence speed. CityLight not only has a relatively high convergence speed but also exhibits a stable and consistent superiority over all state-of-the-art methods.

C.7 Time Consumption Analysis

Table 8 provides a detailed comparison of the computational time cost of CityLight against all baselines in the same experimental environments. FRAP, CoLight, and Advanced-Colight assign each agent one independent policy network, thereby having an extremely high resource demand when the number of agents scales to the thousand level. Therefore, we do not include them in city-level performance evaluations. Concerning LLMLight, we adopt GPT-4o-mini as the basic large



Figure 9: Visualizations of cases of road networks and intersections in our datasets. The blue line denotes roads and the green point denotes intersections.

Model	Manhattan		Chaoyang		Central Beijing	
	TP \uparrow	ATT \downarrow	TP \uparrow	ATT \downarrow	TP \uparrow	ATT \downarrow
Fixed Time	2343 \pm 0	1687.5 \pm 0	6076 \pm 0	826.7 \pm 0	18602 \pm 0	1514.9 \pm 0
Max Pressure	2731 \pm 0	1587.8 \pm 0	1215 \pm 0	1776.1 \pm 0	5448 \pm 0	1879.9 \pm 0
Adjusted Max Pressure	3371 \pm 0	1499.1 \pm 0	5909 \pm 0	785.3 \pm 0	<u>18950 \pm 0</u>	<u>1497.4 \pm 0</u>
FRAP	1957 \pm 110	1682.1 \pm 20.3	6188 \pm 48	920.1 \pm 31.4	17156 \pm 109	1575.8 \pm 18.1
CoLight	3480 \pm 27	1519.3 \pm 8.2	6661 \pm 31	758.2 \pm 18.5	18584 \pm 189	1490.8 \pm 22.3
MPLight	3136 \pm 39	1574.7 \pm 12.1	6104 \pm 38	888.2 \pm 22.9	17535 \pm 202	1550.4 \pm 25.7
Efficient-MPLight	2819 \pm 49	1636.0 \pm 15.5	5916 \pm 41	964.6 \pm 24.5	16063 \pm 173	1592.3 \pm 21.1
Advanced-CoLight	<u>3523 \pm 31</u>	<u>1514.9 \pm 13.8</u>	<u>6730 \pm 22</u>	<u>749.3 \pm 13.2</u>	17608 \pm 155	1548.3 \pm 14.8
Advanced-MPLight	3339 \pm 37	1547.9 \pm 17.5	6347 \pm 39	814.3 \pm 22.6	16691 \pm 171	1578.2 \pm 18.9
GPLight	3091 \pm 25	1588.6 \pm 12.8	5892 \pm 36	949.1 \pm 23.1	17499 \pm 131	1580.8 \pm 15.5
LLMLight	2325 \pm 0	1716.7 \pm 0	1835 \pm 0	1653.6 \pm 0	7568 \pm 0	1828.2 \pm 0
CityLight (Ours)	3962 \pm 17	1422.9 \pm 10.8	7702 \pm 25.2	599.5 \pm 16.9	21548 \pm 137	1437.9 \pm 14.9
Improvement	12.46%	6.07%	14.45%	23.65%	13.71%	3.97%

Table 6: Average performances on three random seeds in three region-scale datasets. Bold denotes the best results and underline denotes the second-best. TP and ATT are short for throughput and average travel time.

language agent. As we have to make decisions for every agent every 15 seconds during the one-hour episode, the overall requirement on LLM calls is substantial and leads to considerable API using costs. Therefore, we also only evaluate LLMLight on region-level datasets. Overall, the training time requirements for CityLight in different datasets are comparable to existing parameter-sharing methods and are quite acceptable.

D. Theoretical Analyses

In our method, we adopt the full parameter-sharing framework, MAPPO, to generate a universally applicable policy for heterogeneous intersections with intricate between-intersection interactions. Through our experiments, we found that such full parameter-sharing training is effective across different intersection configurations and the entire city, with superiority over assigning each configuration one parameter-sharing policy network and assigning each sub-region one parameter-sharing policy network. Here we present some

theoretical analyses of how to explain such a phenomenon.

Proposition 1 (Full Parameter Sharing in TSC) *When controlling traffic signals in N intersections with N individual agents, full parameter sharing among all agents may be the optimal parameter-sharing strategy.*

Considering an arbitrary grouping strategy that divides the N agents into n groups, where the policy and state value function of group i is denoted as π^i and $V_{\pi^i}^i(s)$, respectively. We have:

$$V_{\pi^i}^i(s) = \mathbb{E}_{a^i \sim \pi^i(a^i|s)} [r^i(s, a^i) + \gamma V_{\pi^i}^i(s')]. \quad (8)$$

The global state value function is the sum of all local state value functions as:

$$\mathbf{V}_{\{\pi^1, \dots, \pi^n\}}(s) = \sum_i V_{\pi^i}^i(s). \quad (9)$$

We eliminate (s) for short in the following analyses.

Considering a learning algorithm that approximates the optimal policy π_* with π_+ regarding a given state value

Model	Jinan		Beijing	
	TP \uparrow	ATT \downarrow	TP \uparrow	ATT \downarrow
Fixed Time	33681 \pm 0	1605.2 \pm 0	60615 \pm 0	1133.5 \pm 0
Max Pressure	2492 \pm 0	2051.7 \pm 0	15563 \pm 0	1566.7 \pm 0
Adjusted Max Pressure	33367 \pm 0	1601.8 \pm 0	64613 \pm 0	1090.3 \pm 0
MPLight	30476 \pm 203	1633.0 \pm 18.9	60652 \pm 144	1145.9 \pm 28.1
Efficient-MPLight	29249 \pm 188	1659.4 \pm 15.8	57826 \pm 111	1164.6 \pm 24.3
Advanced-MPLight	33800 \pm 169	1608.7 \pm 16.2	64764 \pm 72	1088.2 \pm 17.5
GPLight	29899 \pm 178	1660.1 \pm 18.2	60250 \pm 108	1149.8 \pm 25.1
CityLight (Ours)	36742 \pm 108	1553.6 \pm 11.9	70451 \pm 55	1030.1 \pm 15.5
Improvement	8.70%	3.01%	9.05%	5.34%

Table 7: Average performances on three random seeds in two city-scale datasets. Bold denotes the best results and underline denotes the second-best. TP and ATT are short for throughput and average travel time.

Method	Manhattan	Chaoyang	Central Beijing	Jinan	Beijing
FRAP	~2 hours	~1.5 hours	~12 hours	-	-
CoLight	~4 days	~2 days	~4 days	-	-
MPLight	~5 hours	~4 hours	~8 hours	~8 hours	~10 hours
Efficient-MPLight	~4.5 hours	~3.5 hours	~7 hours	~8 hours	~8 hours
Advanced-Colight	~4 days	~3 days	~6 days	-	-
Advanced-MPLight	~6.5 hours	~4.5 hours	~7.5 hours	~6 hours	~8 hours
GPLight	~14 hours	~12 hours	~14 hours	~17 hours	~18 hours
LLMLight	~4 hours	~2 hours	~17hours	-	-
CityLight	~9 hours	~7 hours	~12 hours	~11 hours	~14 hours

Table 8: Training time consumption of our CityLight model and baseline solutions. '-' denotes no result due to extremely high resource demand or API costs.

function \hat{V}_π , where

$$\pi_* = \operatorname{argmax}_\pi \hat{V}_\pi \quad (10)$$

The algorithm's capability of approximation is denoted as:

$$\hat{V}_{\pi_*} - C_R \leq \hat{V}_{\pi_+} \leq \hat{V}_{\pi_*} - C_L, \quad (11)$$

which holds for $\forall s$ with the constants

$$0 \leq C_L \leq C_R. \quad (12)$$

When the parameters are globally shared among all agents, the learned policy

$$\bar{\pi}_+ = \bar{\pi}_+^1 = \dots = \bar{\pi}_+^n \quad (13)$$

and the optimal policy

$$\bar{\pi}_* = \bar{\pi}_*^1 = \dots = \bar{\pi}_*^n = \operatorname{argmax}_\pi \mathbf{V}_{\{\pi, \dots, \pi\}} \quad (14)$$

satisfies

$$\mathbf{V}_{\{\bar{\pi}_*, \dots, \bar{\pi}_*\}} - C_R \leq \mathbf{V}_{\{\bar{\pi}_+, \dots, \bar{\pi}_+\}} \leq \mathbf{V}_{\{\bar{\pi}_*, \dots, \bar{\pi}_*\}} - C_L, \quad (15)$$

where

$$\mathbf{V}_{\{\bar{\pi}_*, \dots, \bar{\pi}_*\}} = \sum_i V_{\bar{\pi}_*}^i \quad \mathbf{V}_{\{\bar{\pi}_+, \dots, \bar{\pi}_+\}} = \sum_i V_{\bar{\pi}_+}^i. \quad (16)$$

When the parameters are locally shared among agents within each group, the learned policies

$$\pi_+^1, \dots, \pi_+^n \quad (17)$$

and optimal policies

$$\pi_*^i = \operatorname{argmax}_\pi V_\pi^i \quad (18)$$

satisfy

$$V_{\pi_*^i}^i - C_R \leq V_{\pi_+^i}^i \leq V_{\pi_*^i}^i - C_L. \quad (19)$$

Having

$$\mathbf{V}_{\{\pi_*^1, \dots, \pi_*^n\}} = \sum_i V_{\pi_*^i}^i \quad \mathbf{V}_{\{\pi_+^1, \dots, \pi_+^n\}} = \sum_i V_{\pi_+^i}^i, \quad (20)$$

we can obtain

$$\mathbf{V}_{\{\pi_*^1, \dots, \pi_*^n\}} - nC_R \leq \mathbf{V}_{\{\pi_+^1, \dots, \pi_+^n\}} \leq \mathbf{V}_{\{\pi_*^1, \dots, \pi_*^n\}} - nC_L \quad (21)$$

by summing up Eq. (19) over $i = 1, \dots, n$.

Traffic signal control for large-scale intersections is a relatively uniform task where the common goal is to maximize the overall traffic efficiency and there isn't mutual conflict and competence among intersections. Therefore, we may infer that some similarities exist for agents in traffic signal control. Considering the similarities among agents, the optimal policy with global parameter sharing, i.e., $\bar{\pi}_*$, may approximate individual optimal policies, i.e., π_*^i , as:

$$V_{\pi_*^i}^i - L_R \leq V_{\bar{\pi}_*}^i \leq V_{\pi_*^i}^i - L_L, \quad (22)$$

which holds for $\forall s$ with the constants

$$0 \leq L_L \leq L_R. \quad (23)$$

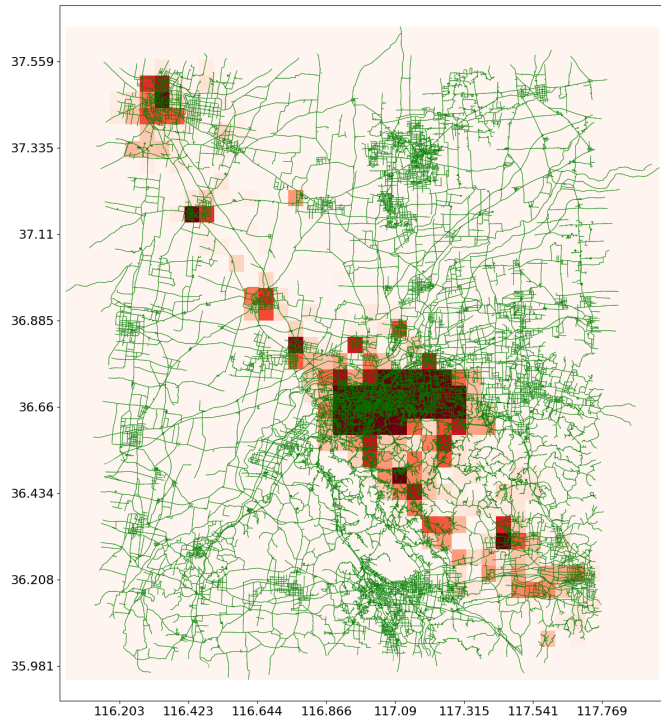
Combining Equ (15) (21) (22), we can obtain that when:

$$L_L \leq C_L - \frac{1}{n}C_R, \quad (24)$$

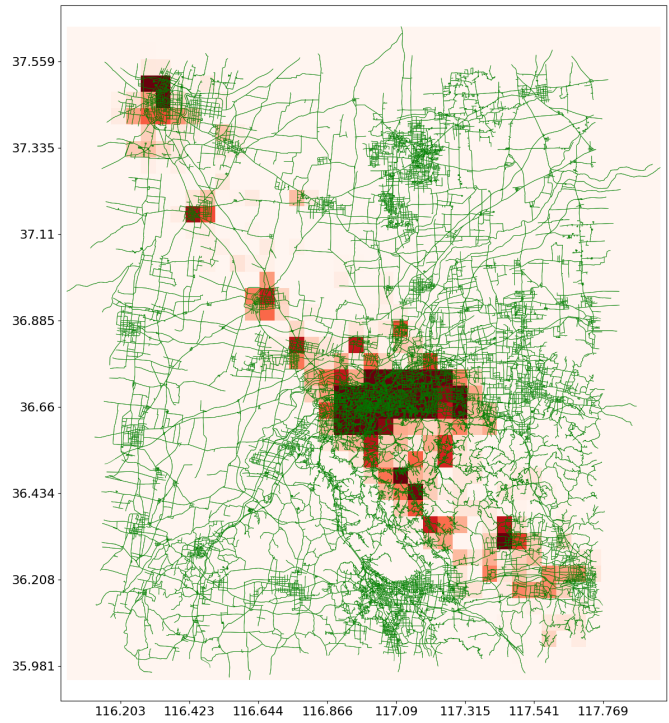
we have

$$\mathbf{V}_{\{\pi_+^1, \dots, \pi_+^n\}} \leq \mathbf{V}_{\{\bar{\pi}_+, \dots, \bar{\pi}_+\}}, \quad (25)$$

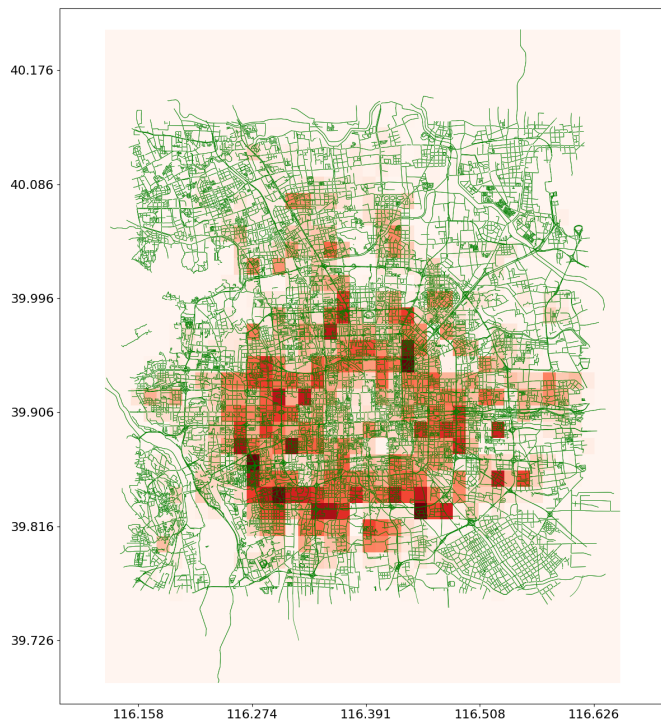
indicating that the policy learned by full parameter-sharing among all agents outperforms policies learned locally within each group.



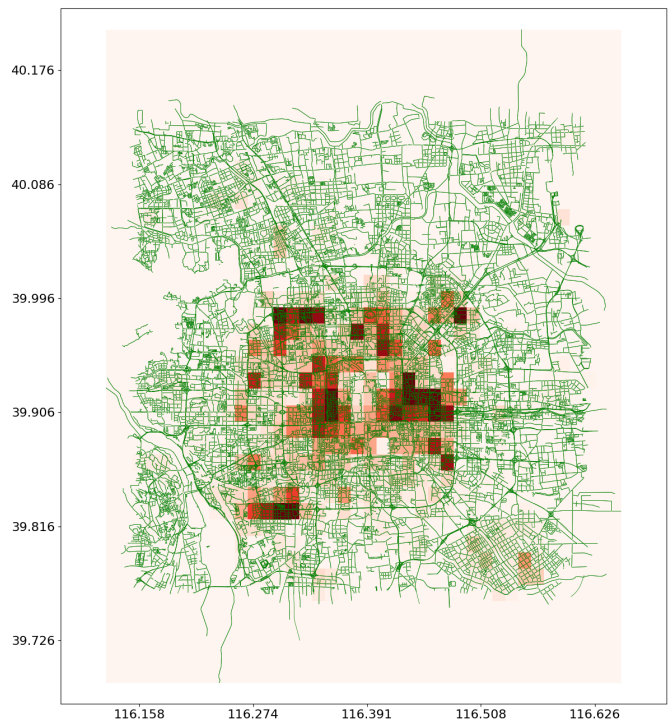
(a) Jinan Origin



(b) Jinan Destination



(c) Beijing Origin



(d) Beijing Destination

Figure 10: Origin-destination distribution of the traffic trajectories in Jinan and Beijing datasets.

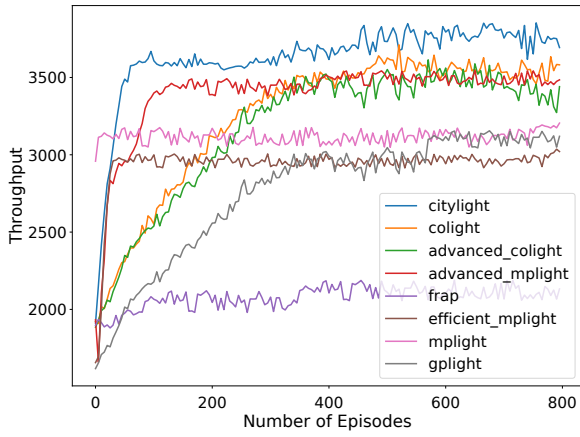


Figure 11: Training curve comparisons. Since the rewards of different methods are not uniform, we visualize the distribution of the throughput metric as the number of episodes increases.